Supplemental Information

Supplemental Figures

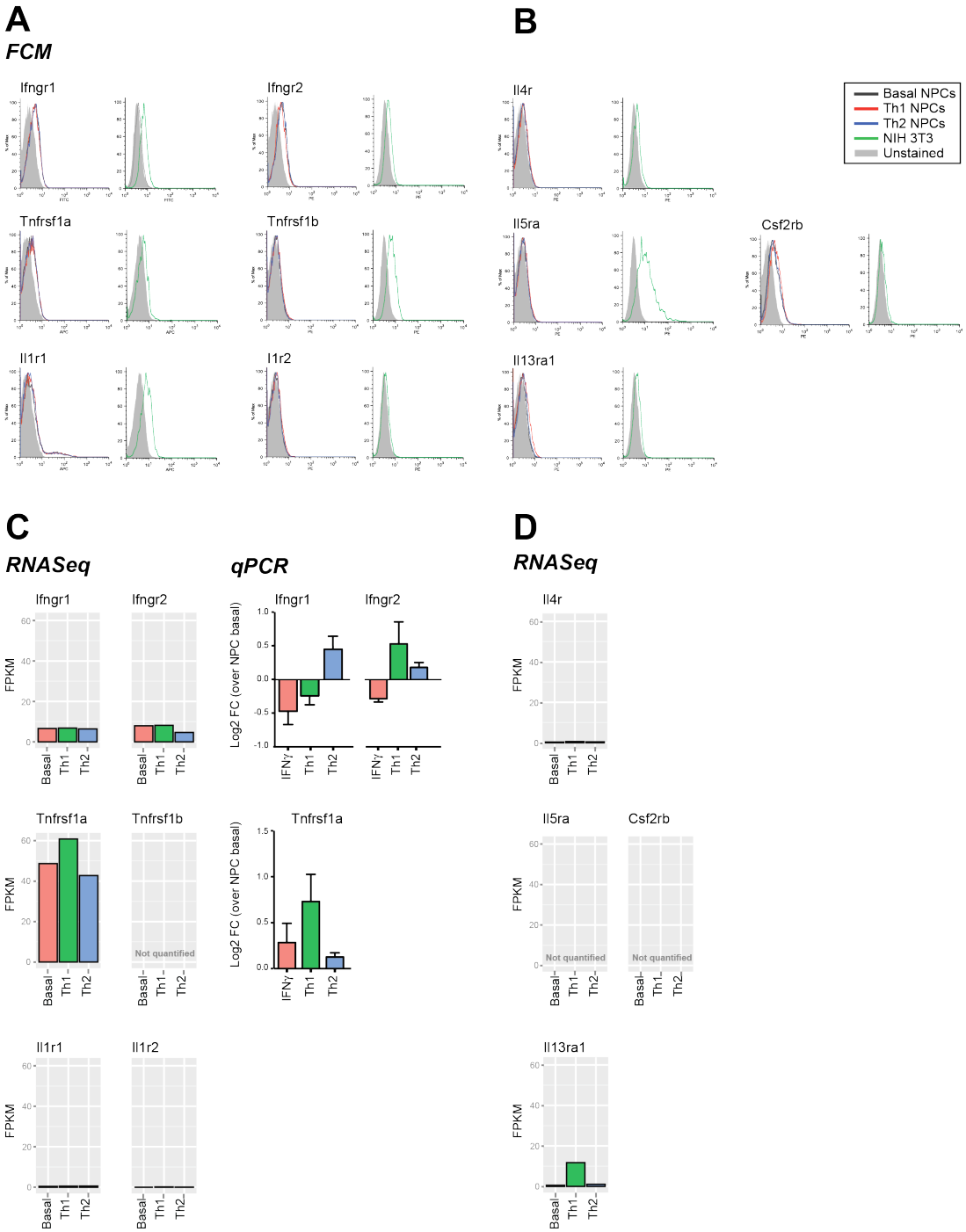

Figure S1. Expression of receptors for Th1 and Th2 cytokines in NPCs and NIH 3T3; related to Figure 1 and **2.** (A-B) FCM analyses. (C-D) mRNA analyses by either RNA-seq (also accessible via GEO [GSE33527]) or qPCR (when mRNA detected). qPCR data in C are expressed as mean log2 fold change (FC) (± SEM) from a total of n = 3 independent experiments.

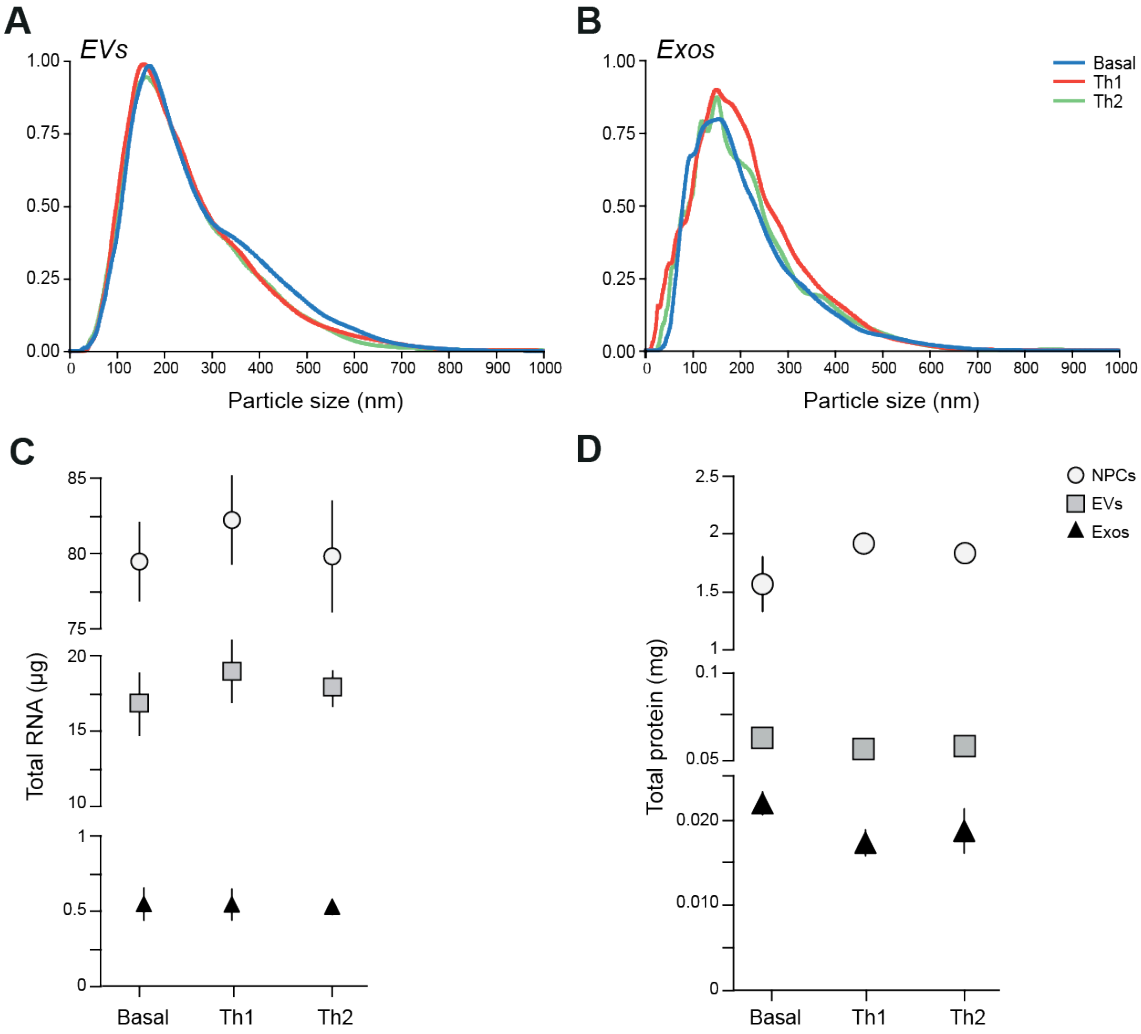

Figure S2; related to Figure 1 and **2.** (A-B) NTA of particle-size distribution in EVs (A) and Exos (B) derived from NPCs grown in Basal (blue), Th1 (red) or Th2 (green) media. Data are mean normalized values from n = 4 independent replicates. Normalization of the data was made by dividing the concentration value at every particle size in the distribution by the largest concentration value within the distribution. (C) Total RNA quantification from 12 x 10^6 NPCs, or associated EVs or Exos, grown as in A-B. (D) Total Protein quantification from 12 x 10^6 NPCs, or associated EVs or Exos, grown as in A-B. Data in C-D are expressed as mean values (± SEM) from n = 3 independent experiments.

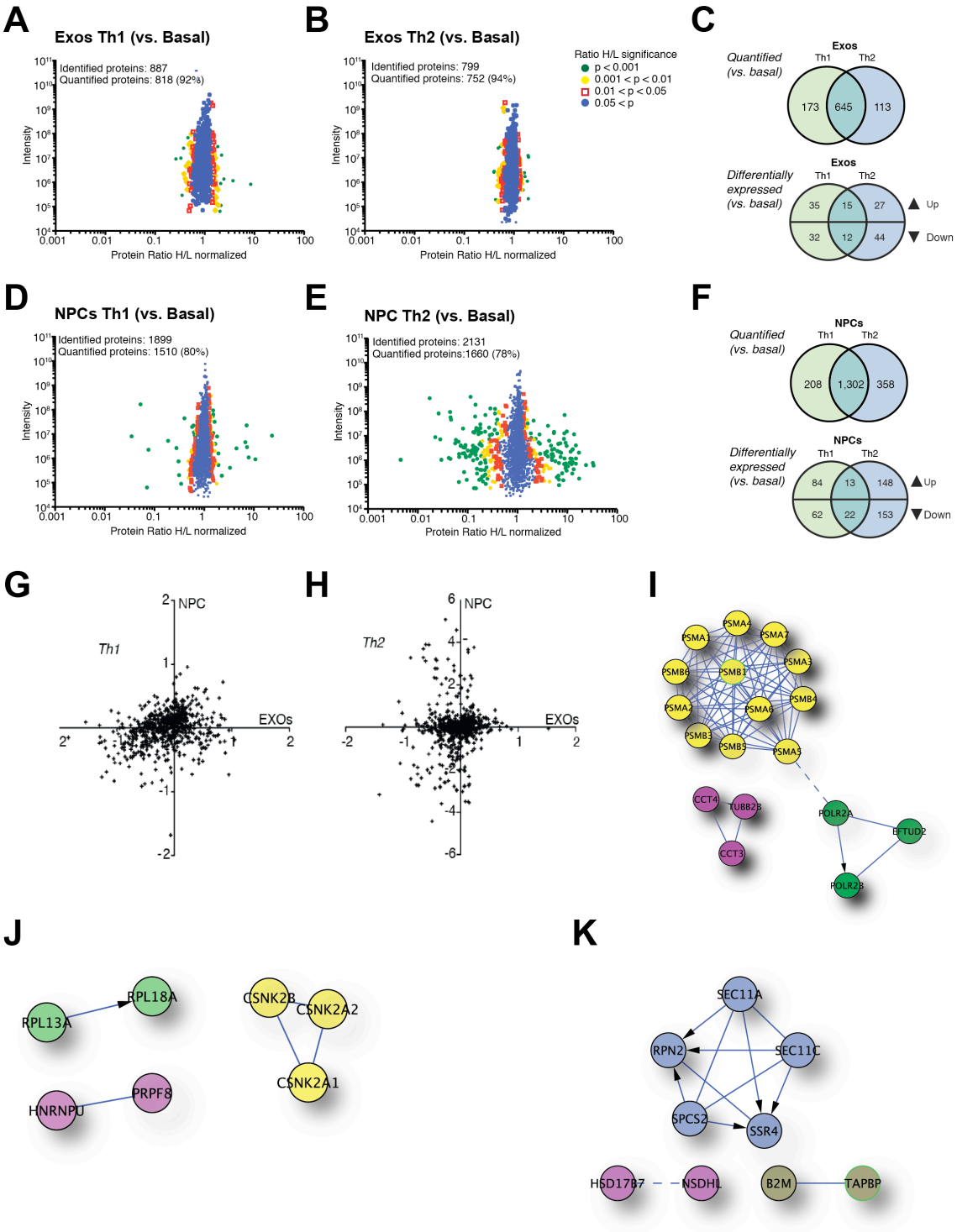

Figure S3. SILAC quantification of proteins expressed in Th1 and Th2 NPCs and Exos; related to Figure 1 and **2.** (A-B) Scatter plots of the identified and quantified proteins in Exos together with a color-coded quantitation significance as provided by MaxQuant software. Protein ratios are plotted against summed peptides intensities. (C) Venn diagrams of the numerical values for the indicated common and unique proteins quantified and differentially expressed in Th1 (green) and Th2 Exos (blue), *vs.* Basal. p≤ 0.05. (D-E) Scatter plots of the identified and

quantified proteins in NPCs together with a color-coded quantitation significance as provided by MaxQuant software. Protein ratios are plotted against summed peptides intensities. (F) Venn diagrams of the numerical values for the indicated common and unique proteins quantified and differentially expressed in Th1 (green) and Th2 NPCs (blue), *vs.* Basal NPCs. $p \leq 0.05$. (G) Scatter plot showing the fold changes of proteins quantified by SILAC in Th1 Exos (*vs*. Basal, x-axis) compared to the fold changes in Th1 NPCs (*vs*. Basal, y-axis). (H) As in E for Th2. (I-K) Constructed FI networks of the highly interacting most significantly up-regulated proteins ($p \leq 0.05$) are showed with activating/catalysing (arrows) or predicted (dashed line) connections based on the protein-protein physical interactions in Th1 EVs (I), Exos (J), and NPCs (K).

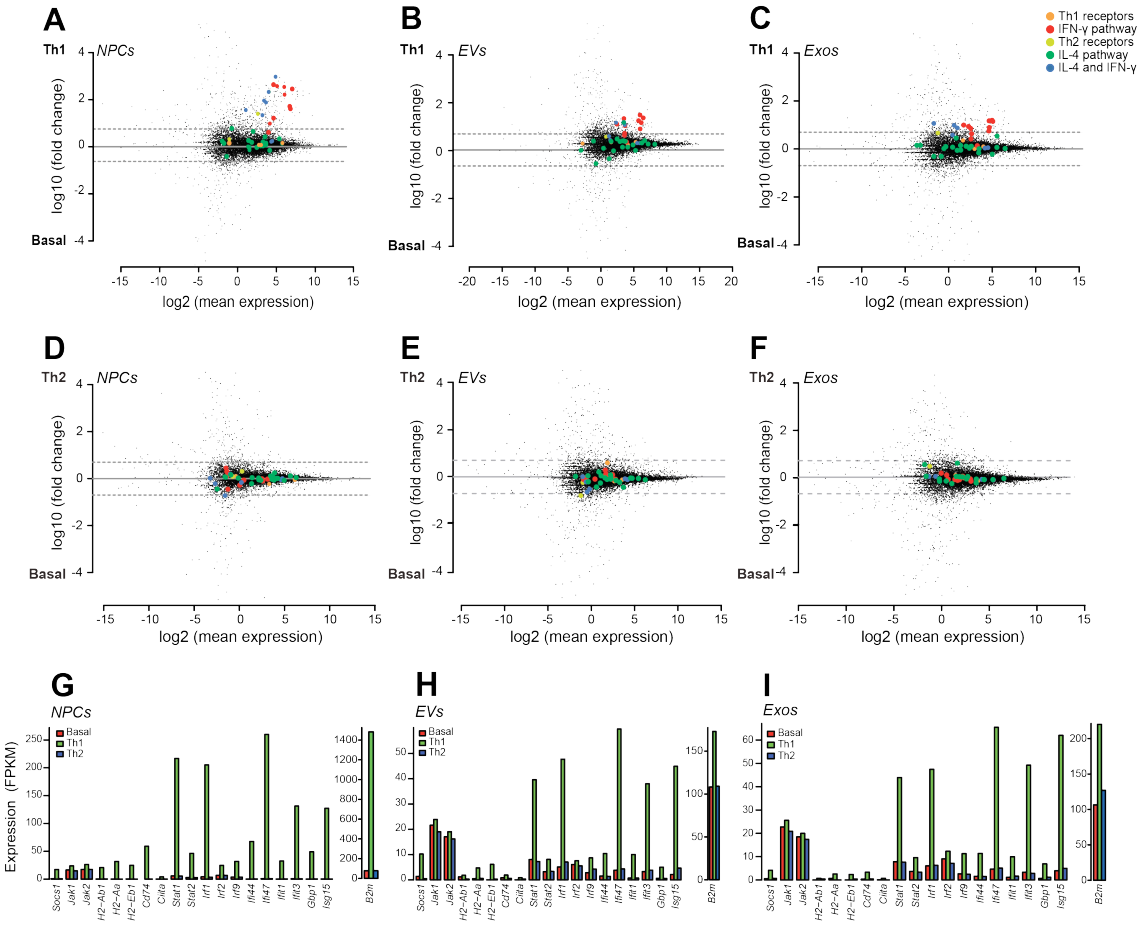

Figure S4; related to Figure 2 (A-C) MA plot of Th1 NPCs, EVs and Exos *vs.* Basal. (D-F) MA plot of Th2 NPCs, EVs and Exos (*vs.* Basal). The x-axis is the $\log_2$ mean expression between Basal and Th1, while the y-axis is the $\log_{10}$ fold change between Th1 and Basal. The y-axes scales have been limited excluding fold changes at the extremes. Genes belonging to manually curated gene sets were highlighted: Th1 receptors (*IFNgR1, IFNgR2, TNFRsf1a, IL-1R1*); IFN-γ pathway (*Stat1, Stat2, Irf1, Irf2, Irf9, Ifi44, Ifi47, Ifit1, Ifit3, Gbp1, Isg15*); Th2 receptors (*IL-4Ra, IL-13Wa1*); IL-4 and IFN-γ pathway (*Socs1, Jak1, Jak2, H2-Ab1, H2-Aa, H2-Eb1, Cd74, Ciita*); IL-4 pathway (*Src, Tyk2, Shc1, Irs1, Irs2, Irs4, Inpp5d, Grb2, Ecm1, Sos1, Sos2, Pik3ca, Pdk1, Rps6kb1, Akt1, Bad, Jak3, Il4i1, Nfil3, Maf, Bhlhe41*). (G-I) Histogram plots showing the expression of selected genes of the IFN-γ pathway (as in A-F) in Basal (red), Th1 (green) and Th2 (blue) NPCs (G), EVs (H) and Exos (I). The y-axis indicates FPKMs for each gene.

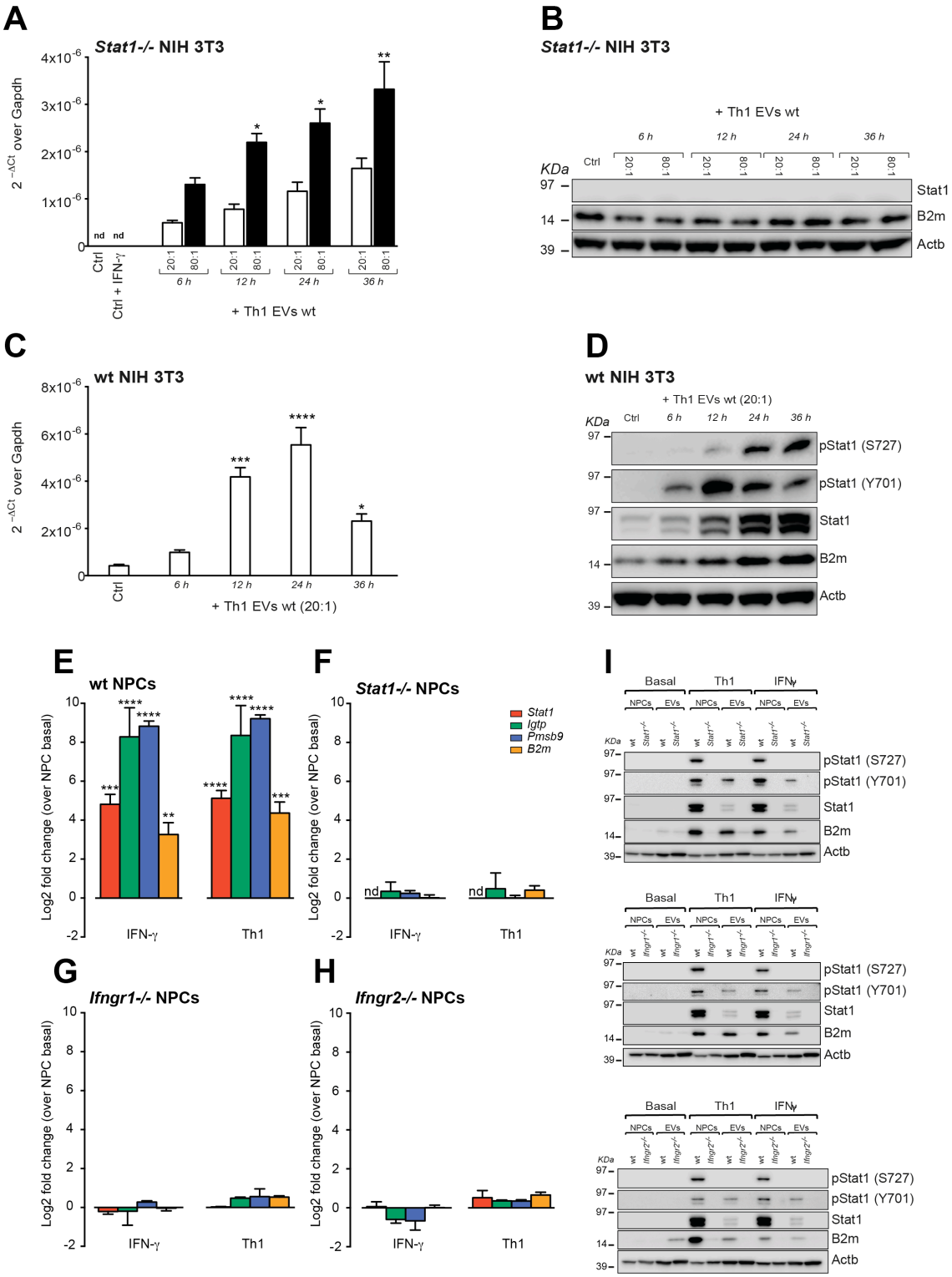

Figure S5. Evidence of the direct transfer of the enriched mRNAs and proteins in Th1 EVs on target cells; **related to Figure 5.** (A) qPCR and (B) Western blot (B) analyses of the levels of Stat1 and key proteins the IFN-γ pathway in *Stat1*$^{-/-}$ target cells treated with two different ratios of wild type Th1 EVs for as long as 36 h in vitro. (C) and (D) are transfer experiments as in A-B, but on wild type target cells. Ctrl are not treated target cells; nd: not

detectable. Real-time data are expressed as mean 2^dCt (± SEM) over Gapdh from a total of n = 3 independent experiments. ****p<0.0001; ***p<0.001; *p<0.05, compared to either 20:1 (A) or Ctrl (C). WB panels are representative of n= 5 independent protein preparations showing the same trends. β-actin (Actb) was used as a loading control.

(E-I) qPCR quantification of the expression of key elements of the Stat1 pathway in wild type (E), *Stat1*$^{-/-}$ (F), *Ifngr1*$^{-/-}$ (G), and *Ifngr2*$^{-/-}$ (H) NPCs treated with either IFN-γ or Th1 cytokine cocktails for 24 hours *in vitro*. Data are expressed as mean log2 fold change (± SEM) over NPC basal from a total of n = 3 independent experiments. ****p< 0.0001; ***p< 0.001; **p< 0.01, compared to NPC basal. nd= not detectable. (I) Western blots of the expression of key elements of the Stat1 pathway in NPCs and EVs as in E-I. These panels are representative of n= 4 independent protein preparations showing the same trends. β-actin (Actb) was used as a loading control.

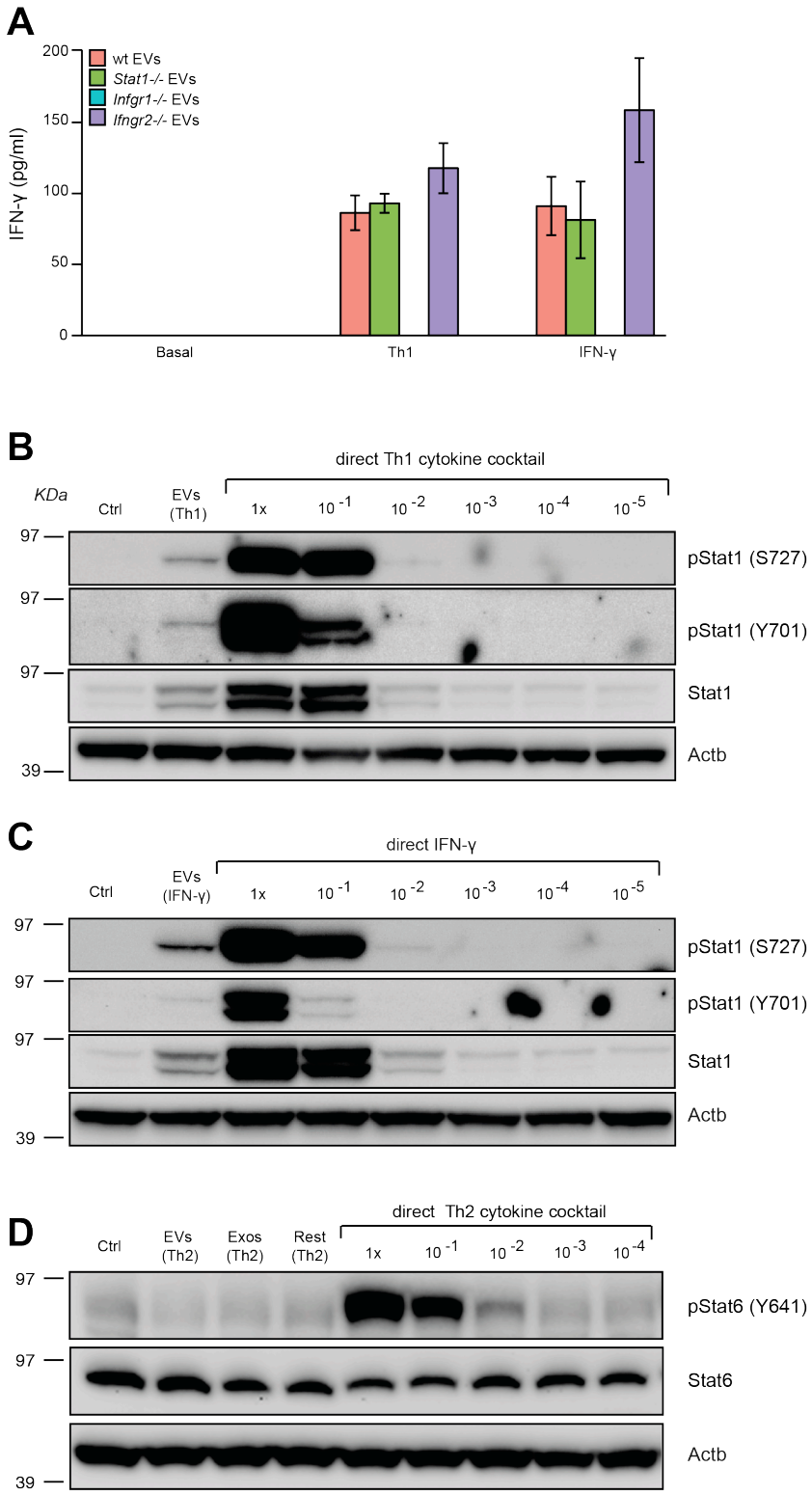

Figure S6; related to Figure 5 and **S5.** (A) Quantification of IFN-γ in EVs collected from 6 x 10^6 wt, *Stat1*$^{-/-}$, *Ifngr1*$^{-/-}$, and *Ifngr2*$^{-/-}$ NPCs. Data are expressed as mean numbers (± SEM) from a total of n= 3 independent EV preparations. (B-C) Western Blot analyses of the Stat1 pathway in target cells exposed to Th1 EVs, or serial dilutions of either the whole Th1 cytokine cocktail (B) or IFN-γ alone (C). (D) Western Blot analyses of the Stat6 pathway in target cells exposed to

EVs, Exos, or serial dilutions of the whole Th2 cytokine cocktail. Panels in B-D are representative of n=3 protein preparations showing same trends. Rest: pool of not-Exosomal fractions (1-5 and 10). β-actin (Actb) was used as a loading control.

Supplemental Tables

Table S1. Identified proteins in NPC, EV and Exo SILAC; related to Figure 2. (A) Identified proteins in EV Th1 SILAC (*vs.* basal). (B) Identified proteins in EV Th2 SILAC (*vs.* basal). (C) Quantified proteins in EV Th1 SILAC with H/L ratio and associated significance. (D) Quantified proteins in EV Th2 SILAC with H/L ratio and associated significance. (E) Proteins significantly up or down regulated ($p \leq 0.05$) in EV Th1 SILAC only with H/L ratio and associated significance. (F) Proteins significantly up or down regulated ($p \leq 0.05$) in EV Th2 SILAC with H/L ratio and associated significance. (G) Proteins significantly up or down regulated ($p \leq 0.05$) both in EV Th1 and Th2 SILAC with H/L ratio and associated significance. (H) Identified proteins in Exo Th1 SILAC (*vs.* basal). (I) Identified proteins in Exo Th2 SILAC (*vs.* basal). (J) Quantified proteins in Exo Th1 SILAC with H/L ratio and associated significance. (K) Quantified proteins in Exo Th2 SILAC with H/L ratio and associated significance. (L) Proteins significantly up or down regulated ($p \leq 0.05$) in Exo Th1 SILAC only with H/L ratio and associated significance. (M) Proteins significantly up or down regulated ($p \leq 0.05$) in Exo Th2 SILAC with H/L ratio and associated significance. (N) Proteins significantly up or down regulated ($p \leq 0.05$) both in Exo Th1 and Th2 SILAC with H/L ratio and associated significance. Colour codes in E-G indicate up regulation (green) or down regulation (red). H/L ratios in C-G correspond to the ratios between Th1/Th2 (H) and basal (L) EVs.

Gene ontology (GO)-based biological process (BP) distribution for proteins identified in EVs Th1 (O), EVs Th2 (P), Exo Th1 (Q) and Exo Th2 (R).

(S) Identified proteins in NPC SILAC Th1 vs. basal. (T) Identified proteins in NPC SILAC Th2 vs. basal. (U) Quantified proteins in NPC SILAC Th1 vs. basal with H/L ratio and associated significance. (V) Quantified proteins in NPC SILAC Th2 vs. basal with H/L ratio and associated (colour-coded) significance. H/L ratios in C-D correspond to the ratios between Th1/Th2 (H) and basal (L) NPCs.

Table S2. Reactome pathways enrichment for NPCs, EVs, Exos Th1 and Th2; related to Figure 2.

Table S3. Microarrays data and analyses; related to Figure 4. (A-C) Target cell gene expression changes as determined by microarray of NIH 3T3 cells following exposure to EVs Basal (A), Th1 (B), or Th2 (C), *vs.* not exposed. (D-E) Target cell gene expression changes as determined by microarray of NIH 3T3 cells following

exposure to EVs Th1 (D) or Th2 (E), *vs.* EVs Basal. (F) List of the quantified leading IDs determined by SILAC for control NIH 3T3 cells with H/M ratio and associated significance, as well as count frequency indicated. (G-I) List of the quantified leading IDs determined by SILAC for target cells exposed to EVs Basal (G), EVs Th1 (H) or EVs Th2 (I) with H/M ratio and associated significance, as well as count frequency indicated. (J) Significantly enriched (FDR< 0.01) GO terms in the Genemania network from genes and proteins differentially expressed in target cells exposed to EVs Basal, *vs.* not exposed. (K) Significantly enriched (FDR< 0.01) GO terms in the Genemania network from differentially expressed genes and proteins common to target cells exposed to EVs Basal, Th1 and Th2, *vs.* not exposed. (L) Significantly enriched (FDR < 0.01) GO terms in the Genemania network from genes and proteins differentially expressed in target cells exposed to EVs Th1, *vs.* EVs Basal. (M) Enriched GO terms in the Genemania network from genes and proteins differentially expressed in target cells exposed to EVs Th2, *vs.* Basal.

Supplemental Movies

Movie S1; related to Figure 3. Z stacks showing uptake of numerous CD63-RFP EVs *in vitro* by farnesylated fGFP (green plasma membrane) target cells. 24h after treatment labelled EVs have translocated into the cytoplasm and appear in more perinuclear regions. Confocal images were adjusted and deconvolution performed to generated movies at 15Hz using the software ImageJ (NIH). Scale bar: 5 μm.

Supplemental Experimental Procedures

NPC preparations

C57BL/6 B6.129S7-*Ifngr*^{tm1Agt}/J (*Ifngr1*$^{-/-}$) mice (Huang et al., 1993) were provided by Burkhard Becher, Institute of Experimental Immunology, Zürich, Switzerland; C57BL/6 IFNgR D/D (*Ifngr2*$^{-/-}$) mice (Kreutzfeldt et al., 2013) were provided by Werner Muller, University of Manchester, United Kingdom; while C57BL/6 *Stat1*$^{-/-}$ mice (Durbin et al., 1996) were provided by Birgit Strobl, University of Veterinary Medicine, Vienna, Austria. NPCs lines were prepared from the subventricular zone (SVZ) of 7-12 week old (18-20 gr) C57BL/6 or SJL wild type (wt) or mice knocked out in key elements of the Jak/Stat1 pathway (as above), as described (Pluchino et al., 2008). Mice were humanely culled by cervical dislocation followed by decapitation. The parietal bones were cut in a way cranial to caudal using micro-chirurgic scissors. The brain was removed and positioned in a Petri dish (Coring Costar) containing sterile PBS 1X. Brain coronal sections were taken 2 mm from the anterior pole of the brain, excluding the optic tracts and 3 mm posterior to the previous cut (using a brain slice matrix). The SVZ of the lateral ventricles was isolated from the coronal section using iridectomy scissors. Tissues derived from at least two mice were pooled to generate each culture. Dissected tissues were transferred to a 15 ml tube with Digestion Medium - Early Balance Salt Solution (EBSS, GIBCO), Papain (1 mg/ml, Worthington), EDTA (0.2 mg/ml, Sigma) and L-cysteine (0.2 mg/ml, Sigma) - and incubated for 45 min at 37°C on a rocking platform. At the end of the incubation, the tube was centrifuged at 1000 rpm for 12 minutes, the supernatant was removed and the pellet was mechanically disaggregated with 2 ml of EBSS. The pellet was centrifuged again at 1000 rpm for 12 minutes and then dissociated with a 200μl pipette and plated in Complete Growth Medium (CGM). CGM is constituted of mouse NeuroCult™ Basal medium plus mouse NeuroCult™ proliferation supplements (Stem Cell Technologies) added with 2 μg/ml heparin (Sigma-Aldrich), 20 ng/ml purified human recombinant Epidermal Growth Factor (EGF; Provitro) and 10 ng/ml human recombinant fibroblast growth factor (FGF)-2 (Provitro). After approximately one week, a small percentage of the isolated cells begun to proliferate, giving rise to small cellular aggregates, which are similar to rounded spheres (called neurospheres) and which grow in suspension. When neurospheres reached the necessary dimension (150-200 μm diameter), the cells were harvested in a 15 ml tube (Falcon) and centrifuged at 800 rpm for 12 minutes. The supernatant was then removed, 200 μl was left and the pellet was mechanically dissociated (e.g., by forcing the pellet repeatedly through a sterile tip, until a single cell

suspension was obtained). For the subsequent passaging after establishment of the line, NPCs were grown in CGM. At time of passaging (every 3-5 days), neurospheres were dissociated by enzymatic digestion with Accumax™ (Sigma) at 37°C for 15 min, the number of viable cells determined by trypan blue exclusion and viable cells re-plated at 8000 cells/cm^2. NPCs at passage n≤ 15 were used in all experiments.

NIH 3T3 cell cultures

For routine expansion, NIH 3T3 cells were expanded in complete high glucose and sodium pyruvate Dulbecco's Modified Eagle Medium (DMEM, Gibco), containing 10% FBS, 2 mM glutamine, 1 mM penicillin, 100 μg/ml streptomycin, as previously described (Pluchino et al., 2009). Cells were sub-cultured using 0.05% Trypsin-EDTA (Gibco), and maintained at 37°C in a humidified atmosphere of 5% CO_2 in air.

NIH 3T3-like cell lines were generated from the kidneys of C57BL/6 B6.129S7-*Ifngr*^{tm1Agt}/J (*Ifngr1*$^{-/-}$), C57BL/6 IFNgR D/D (*Ifngr2*$^{-/-}$) and C57BL/6 *Stat1*$^{-/-}$ mice by means of serial passaging until spontaneous immortalization.

Th1 and Th2 cytokine cocktails and treatments

NPCs were dissociated with Accumax™ (Sigma), as described before, and plated 1.2 x 10^6 cells/ml in CGM with or without either Th1 (500 IU/ml recombinant mouse IFN-γ, BD Biosciences; 200 UI/ml recombinant mouse TNF-α, Pepro Tech Inc.; 100 UI/ml recombinant mouse IL-1β, Euroclone) or Th2 (10 ng/ml recombinant murine IL-4, R&D; 10 ng/ml recombinant mouse IL-5, R&D; 10 ng/ml recombinant mouse IL-13, R&D) cytokine mixes for 16 hours in vitro, as described (Pluchino et al., 2008). At the end of the conditioning, NPCs were harvested and the supernatants processed for the collection of either EVs or Exos.

NIH 3T3 cells were plated 3 x 10^5 cells/well (6 well plates) in DMEM containing 10% FBS (as above) without either 1X Th1 or Th2 cytokine mixes, or with 10-fold serial dilutions (from 10^{-1}X to 10^{-5}X) for 16 hours in vitro. At the end of the conditioning NIH 3T3 cells were harvested and processed for the collection of protein extracts.

Electron microscopy

NPCs or EVs were washed in 0.1 M phosphate buffer and fixed in 3.5% glutaraldehyde. Floating NPCs or EVs were re-suspended in 2% agar, while adherent cell cultures were processed on chamber slides. For transmission electron microscopy (TEM), fixed NPCs or EVs were washed, post-fixed in 2% osmium, dehydrated and

embedded in Durcupan resin (Fluka). 1.5 μm-thick semithin sections were cut with a diamond knife, mounted onto slides and counterstained with 1% toluidine blue. Sections containing cells or EVs were re-embedded in resin for ultrathin sectioning (70 nm) and analysis was performed under the Tecnai Spirit G2, FEI microscope using a Morada camera (Soft Imaging System, Olympus). For GFP pre-embedding immunogold, adherent cell cultures were fixed in 4% paraformaldehyde 0.5% glutaraldehyde, washed, blocked in 0.3% bovine serum albumin-c (BSA-c, Aurion, Netherlands) and incubated in primary antibody (chicken anti-GFP, Aves Labs, 1:200) for 72 h. Then, samples were blocked in 0.5% BSA-c 0.1% fish gelatine and incubated in colloidal gold conjugated secondary antibody (UltraSmall, Aurion, 1:50) for 24 h. Silver enhancement was performed and samples were immersed in 0.05% gold chloride for gold-toning. Samples were then postfixed in 2% glutaraldehyde, contrasted with 1% osmium and processed for TEM.

For negative staining, floating EVs were placed on grids, stained with 2% uranyl acetate, washed and examined under the TEM. For scanning electron microscopy (SEM), NPCs were fixed in 3.5% glutaraldehyde, washed in PB, postfixed in 2% osmium, and dehydrated in ethanol on glass coverslips. Samples were critical point dried with carbon dioxide, fixed to aluminium stubs, sputter coated and examined under the SEM (S-4100, Hitachi).

EV sizing and phenotype by flow cytometry (FCM) analysis

The size of EVs was determined by BD FACSCanto II system (Becton Dickinson Biosciences). The instrument was rinsed extensively with 0.1 μm filtered particle-free rinse solution to eliminate the background. 1 μm beads (Molecular Probes) were used as size markers, and analysis was performed using a logaritmic scale for forward scatter and side scatter parameters. 100 μl of stained EVs were diluted in a final volume of 500 μl and were analysed by Flow Cytometry (FCM) during 130-second acquisition time. FCM analysis was performed using PE conjugated anti CD9 (clone eBioKMC8; eBiosciences), PE anti VLA4 (clone PS/2), PE anti CD44 (clone IM7) or a PE labeled Rat IgG2a or IgG2b isotype control at a final concentration of 0.25 ng/μl.

Nanoparticle Tracking Analysis (NTA)

Samples were diluted 1:1000 with PBS. 5 repeated measurements of 200 seconds were recorded consecutively for each sample and were analysed using a Nanoparticle Tracking Analysis (NTA) instrument (LM10HSBF, NanoSight ltd) fitted with a 60 mW,

405 nm laser diode source to illuminate a region of the 250 µl sample introduced into the illumination modules. The temperature was recorded and resultant liquid viscosity calculated by the instrument. The movement of each particle in the field of view (approximately 100 µm x 80 µm) was measured to generate the average displacement (in terms of x and y) of each particle per unit time. From this measurement, the particle diffusion coefficient was estimated and the hydrodynamic diameter calculated through application of the Stokes-Einstein equation. Data normalisation was made by dividing the concentration value at every particle size in the distribution by the largest concentration value within the size distribution - as a result everything becomes a % of 1 and then the y axis automatically loses its units.

Protein extraction and quantification

Whole cell pellets were solubilised in RIPA buffer (10 mM Tris HCl pH 7.2, 1% v/v Sodium Deoxycholate, 1% v/v Triton X-100, 0.1% v/v SDS, 150 mM NaCl, 1 mM EDTA pH 8) in presence of Complete Protease Inhibitor Cocktail (Roche) and Halt Phosphatase Inhibitor Cocktail (Pierce). EV and Exo pellets were solubilised in RIPA buffer with 3% v/v SDS. Protein quantification was performed using the Bio-Rad DC Protein Assay Kit II.

Western blot analysis

Samples were separated by SDS-PAGE using 10% precast NuPAGE Bis/Tris gels (1.5 mm thickness) under reducing (Reducing Buffer, 10X) and non reducing conditions and MES running buffer and then transferred onto Polyvinylidene fluoride PVDF membranes (0.45 µm pore size, Immobilon) using XCell II Blot Module and NuPAGE transfer buffer (Invitrogen). Loading and transfer were analysed by Ponceau staining the membranes or mini gels staining with SimplyBlue SafeStain (Invitrogen). For immunoblot analysis, membranes were blocked 1 hour at room temperature with Tris-buffered saline/Tween (TBST 10 mM Tris-HCl pH 8.0, 150 mM NaCl, 0.1% Tween 20) containing 5% non fat dry milk and then incubated with primary antibodies over/night at 4°C. After washing with TBST, the filters were incubated with the appropriate horseradish-peroxidase-conjugated secondary antibodies (Thermo Scientific) for 1 hour at room temperature. Immunoreactivity was revealed by using an ECL prime detection kit (Pierce). Primary antibodies used: rabbit polyclonal anti-TNFR1, rabbit monoclonal anti-beta 2 Microglobulin, rabbit polyclonal anti-Stat6 and rabbit polyclonal anti-phospho Stat6 (Tyr641) (Abcam); rat monoclonal anti-CD9 and rat monoclonal

anti-IFN-γ (BD Pharmingen); mouse monoclonal anti-AIP-1/Alix (BD transduction lab); goat polyclonal anti-TSG101 (Santa Cruz); rat monoclonal anti-CD63 (MBL); rabbit monoclonal anti-AGO1, rabbit monoclonal anti-AGO2, rabbit monoclonal anti-HSP90, rabbit polyclonal anti-HSP70, rabbit polyclonal anti-phospho Stat1 (Tyr701), rabbit polyclonal anti-phospho Stat1 (Ser727), rabbit polyclonal anti-Stat1, rabbit polyclonal anti-phospho Jak1 (Tyr1022/1023), rabbit polyclonal anti-phospho Jak2 (Tyr1007/1008), rabbit monoclonal anti-Jak1 and rabbit monoclonal anti-Jak2 (Cell Signalling); mouse monoclonal anti-beta-Actin (Sigma). Molecular weight marker: full-range rainbow (GE Healthcare, Amersham) and SeeBlue Plus2 (Invitrogen).

Stable isotope labelling of amino acids in cell culture (SILAC)

NPCs were cultured in D-MEM/F-12 supplemented with heavy (Arg-13C6, 15N4 and Lys-13C6, 15N2) and light (Arg-12C6, 14N4 and Lys-12C6, 14N2) amino acids (AAs) for at least five doublings *in vitro*. Incorporation rate of the heavy amino acids after five doublings was tested and appeared to be in accordance with the isotopic purity of the heavy amino acids. 1:1 mixing (in terms of total protein content) of normal and conditioned samples was performed before gel loading of SILAC samples. The very same protocol was used for the analysis of NPCs, EVs and Exos Th1 (heavy AAs) *vs.* Basal (light AAs) and Th2 (heavy AAs) *vs.* Basal (light AAs).

NIH 3T3 cells were cultured in custom D-MEM (Lysine/Arginine/Glutamine depleted, Invitrogen) supplemented with heavy (Arg-$^{13}C_6$,$^{15}N_4$ and Lys-$^{13}C_6$,$^{15}N_2$) and medium (Arg-$^{13}C_6$ and Lys-$^{2}H_4$) amino acids (see Table below for further details) for at least five doublings *in vitro*. Incorporation rate of the heavy amino acids after five doublings was tested and appeared to be in accordance with the isotopic purity of the heavy amino acids (data not shown). 1:1 mixing based on cell number (2.5 million each) of control and EV-exposed samples was performed prior to protein extraction and fractionation. Fractionation was performed with Qiagen Qproteome Cell Compartment kit, collecting cytosolic, membrane, nuclear and cytoskelatal fractions that were loaded onto SDS PolyAcrylamide Gel Electrophoresis (PAGE) precasted 4-12% gels (Life Technologies). Gel slices were excised from the gel, sampling the entire length of the lanes. Samples were reduced with 10 mM dithiothreitol (DTT), alkylated with 55 mM iodoacetamide and digested overnight with bovine Trypsin (1.25 ng/μl, Roche) as described elsewhere (Shevchenko et al., 1996). The peptide mixtures were cleaned on a StageTip C18 (Proxeon Biosystems), resuspended in 20 μL of 5% formic acid and analysed with LC/MS proteomics. MaxQuant 1.3.0.5 (Cox and Mann, 2008) was used for SILAC

quantitation analysis with default settings. Briefly, 7 ppm as peptide tolerance, 0.5 Da MS/MS tolerance, methionine oxidation and acetyl (protein N-term) as variable modifications, cysteine carbamidomethylation as fixed modification, 2 missed cleavages, Trypsin/P as cleaving agent, 1% FDR, minimum peptide length of 6 amino acids for identification. The latest available Integr8 complete proteome database for Mus musculus and a custom contaminants list deriving from the cRAP repository were used as fasta databases. In-house Mascot Server 2.2.07 (Matrix Science) was used as search engine. Lists of significantly up and down regulated proteins (H/L ratios with p≤ 0.05) were subjected to post-MS bioinformatics systems biology oriented analysis as described (Bachi and Bonaldi, 2008).

List of amino acids and concentration used for SILAC on NIH 3T3 cells.

	Amino acid	***Cat N°***	***Formula***	***MW***	***Final conc. (mM)***	***Weight (mg)/500 ml***
$^{2}H_4$	L-Lys medium 2HCL	489034	$H_2NCH_2(CD_2)_2CH_2CH(NH_2)CO_2H \cdot 2HCl$	223,13	0,798	89
$^{13}C_6, ^{15}N_2$	L-Lys heavy HCL	608041	$H_2{}^{15}N(^{13}CH_2)_4{}^{13}CH(^{15}NH_2){}^{13}CO_2H \cdot HCl$	190,59	0,798	76
$^{13}C_6$	L-Arg medium HCL	643440	$H_2N{}^{13}C(NH)NH{}^{13}CH_2(^{13}CH_2)_2{}^{13}CH(NH_2){}^{13}CO_2H \cdot HCl$	216,62	0,398	43
$^{13}C_6, ^{15}N_4$	L-Arg heavy HCL	608033	$H_2{}^{15}N{}^{13}C(^{15}NH){}^{15}NH(^{13}CH_2)_3{}^{13}CH(^{15}NH_2){}^{13}CO_2H\ HCl$	220,59	0,398	44

Reactome functional interactions

Reactome Functional Interaction (FI) plugin in Cytoscape version 2.8.3 was used to construct a pathway-based protein functional interaction sub-network based on SILAC data set for NPCs, EVs and EXOs under Th1 and Th2 cytokines conditioning. GO based biological process data was obtained from Human Protein Reference Database and mapped onto proteins identified in EXO and EV fractions. As biological annotations are better for human proteins, mouse Swiss-Prot identifiers were converted to NCBI Entrez Gene identifiers and subsequently into human orthologous identifiers by using NCBI Homolgene (in-house Perl scripts).

RNA extraction and quantification

The NPC, EV or Exo pellet was re-suspended in TRIzol® reagent (Invitrogen) for subsequent RNA isolation according to the manufacturer's recommendations. Total RNA quantity and purity were assessed with the NanoDrop 2000c instrument (Thermo Scientific). RNA integrity assessments were performed with a BioAnalyzer 2100 (Agilent, Eukaryotic Total RNA Nano Series II).

RNA Sequencing

Total RNA was purified using Trizol. Purity and integrity were confirmed by BioAnalyser (Agilent). Paired End library construction and poly-A selection were performed by EASIH (The Eastern Sequence and Informatics Hub, University of Cambridge, Cambridge) according to the Illumina standard protocol. Sequencing was performed by EASIH using Illumina GAII. On average we retrieved ~17.2 million 72nt paired-end reads that we pre-processed using the Kraken suite of tools. Reads were trimmed to remove matches to 3' adapter sequence and reads with 5' adapter contamination were discarded. Reads were also trimmed based on quality score and poly-N stretches. Subsequently, reads less than 45 bases in length were removed. Redundant read pairs were collapsed to unique entries and in these cases the maximum base quality at each position was retained. Expression analysis was performed with the Cufflinks package (TopHat v 2.0.4, CuffDiff v2.0.2, Bowtie v2.0.0-beta6) (Trapnell et al., 2012) using Ensembl gene annotation (v66). Fragment statistics for TopHat were estimated by aligning a set of reads sampled from each of the RNA-Seq libraries to a set of Ensembl derived exonic regions (regions from exons, greater than 1000 bases in length, which appear unspliced, or are absent from, the other annotated transcripts spanning a genomic region). The gene set was subsequently filtered to retain only genes with an <OK> status report in all samples. Genes with redundant short name entries, according to Ensembl annotation, were collapsed to a single representative (selected to have the greatest IQR between its associated FPKM values). Genes for whom the mean expression across all samples is greater than the median mean expression value across all genes were retained and genes for which the length of the longest associated transcript fell below the mean fragment length for the experiment (calculated above) were removed. In each pairwise comparison, genes for which all expression values were 0 were excluded. The GO enrichment analysis on genes differentially expressed in NPC Th1 was performed using the topGO package (v. 2.12.0) in R/Bioconductor. The gene list filtered as described above was used as universe, and genes with fold-change >5 or <0.2 were selected. P-values were

calculated using Fisher's exact test with the *classic* algorithm as implemented in topGO. P-values were corrected using the Benjamini-Hochberg method.

Vector production, titration and NPC infection

NPCs were labelled *in vitro* using third-generation lentiviral vectors pCCL.sin.cPPT.hPGK engineered with either *EGFP* at different sub-cellular localization which target the fluorescent protein to the cytoplasm (EGFP), to the inner plasma membrane (farnesylated-EGFP) and to the nucleus (nls-EGFP) respectively (Follenzi et al., 2000); or the tetraspanin CD63 fused to red fluorescent protein (mRFP; appended to the C terminus of CD63) (Artavanis-Tsakonas et al., 2006). Transgene expression was measured by direct fluorescence at least 1 week post-transduction. A Multiplicity of Infection (MOI) of 10 was used for NPCs.

EV transfer experiments on NIH 3T3 cells

NIH 3T3 cells were seeded on glass coverslips in 24-well plates (5 x 10^4 cells per well) and exposed to EVs collected from NPC expressing GFP variants at different sub-cellular localization (EV derived from 1 million NPCs; 20:1 NPC:NIH 3T3 EV ratio) for 24 hours and analysed by either confocal and STED super-resolution microscopy or flow cytometry for the expression of EGFP or RFP. Flow cytometry was performed with a CyAn ADP Analyzer (Beckman Coulter) and data were analysed with FlowJo data analysis software (Tree Star, Ashland/ Miltenyi Biotec is the official European distributor). In some EV transfer experiments for STED super-resolution microscopy, NIH 3T3 cells were transduced with lenti vectors engineered with fEGFP, and exposed to CD63-RFP EV as before.

3T3 NIH cells or immortalized mouse fibroblasts were plated in a 6-well plate at a rate of 3 x 10^5 in a volume of 2 ml per well. The day after, EVs from 6 million NPCs were seeded on top of each well in a volume of 250 μl of 3T3 medium (ratio NPCs from which EVs were collected to fibroblasts ~ 20:1). Cells were incubated for 24h at 37°C. The day after, supernatant was collected for subsequent cytokine and chemokine production analysis. Cells were detached using Trypsin or a scraper, and washed with PBS, then centrifuged at 800 rcf for 5 min for subsequent Western blot analysis.

Microarray analysis on target cells exposed to EVs

Total RNA was amplified and labelled using the SuperScript™ Indirect RNA Amplification System (Invitrogen) and Alexa Fluor 555 Decapack Set (Invitrogen)

according to the manufacturer's instructions. Labelled RNA was hybridised to the NCode™ microarray (Invitrogen) using MAUI® Hybridization System (BioMicro Systems), according to the manufacturer's protocol. Hybridisation solution was pre-warmed to 42 °C and loaded on the microarray chip. The chip then was placed on MAUI® mixer slide assembly and hybridisation proceeded at 42 °C overnight. Slides were scanned at a 5 μm resolution using a DNA microarray scanner (Agilent Technology). Feature extraction was performed using NimbleScan software, with manual grid adjustment and auto spot finding and segmentation. Data were analysed using the Linear Models for Microarray Data (LIMMA) software package via the R Project for Statistical Computing (www.r-project.org). Data were background-corrected, and normalised between arrays (Smyth and Speed, 2003). Differential expression analysis was performed by fitting a linear model of the data to the experimental design matrix and then calculating Bayesian statistics (B statistics; posterior log odds) adjusted for multiple testing using Benjamini-Hochberg analysis (Smyth, 2004).

Functional networks using GeneMANIA

The lists of genes and proteins differentially expressed between Th1 and basal EVs exposed to control 3T3 cells as identified by microarray and SILAC respectively, were used to create interaction networks using GeneMANIA (Mostafavi et al., 2008; Warde-Farley et al., 2010). The network was weighted using the default weighting method, whereby the weighs were assigned to maximise the connectivity between all input genes. Enrichment of gene ontology terms of input genes in the network was carried out using the Functions tab of the GeneMANIA results page. It reports the enriched GO terms along with FDR values, which are corrected using the Benjamini-Hochberg method. The GO terms with FDR < 0.01 were considered significant.

Quantitative Reverse Transcription PCR

RNA was extracted as described above. Residual genomic DNA was removed with the Ambion® TURBO DNA-free™ kit (Life Technologies), according to the manufacturer's instructions. cDNA synthesis was performed using SuperScript™ III First-Strand Synthesis SuperMix for qRT-PCR (Invitrogen), with random hexamers as primers. qRT-PCR was performed with the TaqMan® Universal PCR Master Mix (Applied Biosystems) and TaqMan® Gene Expression Assays for FAM™ Ifngr1, Ifngr2, Tnfrsf1a, Igtp, Psmb9, B2m, Stat1 (Mm00439522 that detects wt Stat1 only and not the mutant truncated version) and VIC® GAPDH probes. Samples were tested in triplicate

on a 7500 Fast Real-Time PCR System (Applied Biosystems) and analysed with the $2^{-\Delta\Delta CT}$ method (Livak and Schmittgen, 2001).

Immunofluorescence and Confocal Microscopy

NPC were dissociated to single cells and seeded in NeuroCult basal medium on matrigel (BD Biosciences)-coated glass cover slips in 24-well plates (5 x 10^4 cells per well). After 24 hours, culture medium was removed and cells were fixed with 4% paraformaldehyde (PFA) 10 min at room temperature (RT), and then rinsed three times with PBS. Fixed cells were incubated for 60 min at RT with a blocking solution to avoid aspecific binding of the antibodies (PBS 1x + 10% normal goat serum, NGS, Sigma). Fixed cells were sequentially incubated for 2 hours at RT with primary antibody [rabbit anti-GFP (1:500, Invitrogen, Molecular Probes) or rat anti mouse monoclonal antibody to LAMP1 (1:200, Novus Biologicals)) in PBS-0.1% Triton X-100-1% NGS and 1 hour at RT with goat anti rabbit IgG AlexaFluor488-conjugated antibody (1:500, Invitrogen, Molecular Probes). The actin cytoskeleton was stained with Rhodamine phalloidin (1:100 Invitrogen, Molecular Probes). The nuclei were counter-stained with 4,6 diamine-2- fenilindole (1 μg/ml, DAPI, Roche). Cells were then washed and mounted with Fluorescent mounting medium (Dako). Samples were examined and photographed using a laser scanning confocal microscope (TCS-SPE; Leica Inc., Wetzlar).

Stimulated emission depletion (STED) super-resolution microscopy

fGFP transduced NIH 3T3 cells were seeded on 13 mm glass coverslips (5 x 10^4 cells per well) for 24 hours then exposed to EVs collected from CD63-RFP transduced NPCs (20:1 NPC:NIH 3T3 EV ratio). Live imaging or imaging of cells fixed with 4% PFA was acquired under confocal plus STED super-resolution microscopy at 1，2，3，4，and 24 hours after EV transfer. STED images were obtained with a Leica TCS SP8 STED microscope. Nuclei were stained with 4',6-diamidino-2-phenylindole (DAPI) and excited with a 405nm. CD63-RFP labeled EVs were excited with 590nm laser, while fGFP labeled NIH 3T3 cells were excited with a 488 nm laser line and depleted by a 592 nm laser line. Confocal and STED images were adjusted and filtered using the software ImageJ (NIH).

Live cell imaging under confocal microscopy

Live imaging was acquired under Zeiss 780 confocal microscopy 24 hours after EV treatment. CD63-RFP labelled EVs were excited with 561nm laser, while fGFP labelled NIH 3T3 cells were excited with a 488 nm laser. Confocal images were adjusted and deconvolution performed to generate movies at 15Hz using the software ImageJ (NIH).

Enzyme-Linked Immunosorbent Assay (ELISA)

ELISA was performed to determine the level of chemokine MCP-2/CCL8 in 3T3 cell supernatant using ELISA kit Mouse MCP-2/CCL8 DuoSet (R&D Systems) according to the manufacturer's instructions. The limit of detection was 31.25 pg/ml.

Quantification of IFN-γ in EVs

To prove that the effect elicited in NIH 3T3 by Th1 EVs was not the result of IFN-γ contamination in EVs, possibly derived from the Th1 cytokine cocktail used to treat the NPCs, we quantified the levels of IFN-γ in EVs and compared the effects of EVs and those of the equivalent detected concentration of IFN-γ on NIH 3T3 target cells. We performed ELISA for IFN-γ (Elisa kit Mouse IFN-γ DuoSet, limit of detection = 31.25 pg/ml, R&D Systems) on EVs from 6 x 10^6 NPCs (**Figure S12**).

We quantified a concentration of IFN-γ in wt, *Ifngr2*$^{-/-}$ and *Stat1*$^{-/-}$ EVs Th1 equal to 86.33 pg/ml, 117.76 pg/ml and 93.03 pg/ml respectively, and in wt, *Ifngr2*$^{-/-}$ and *Stat1*$^{-/-}$ EVs IFN-γ only of 91.1 pg/ml, 158.55 pg/ml (highest value detected) and 81.33 pg/ml, respectively.

As we use to run the ELISA after having resuspended EVs into a final volume of 100 μl, the expected final absolute quantity of IFN-γ present in EVs would be equal to 158.55 pg x 0.1 = 15.85 pg. Then, we did run signalling experiments with EVs from 6 x 10^6 NPCs seeded on 3 x 10^5 NIH 3T3 cells in a total volume of 2.25 ml. Thus, the expected maximal concentration of IFN-γ present in the culture medium is 15.85 pg/2.25 ml = 7.05 pg/ml. IFN-γ has a molar mass of 18 kDa = 18,000 g/mol (as reported by UniProt). Thus, the corresponding molarity is: 7.05 pg/ml/18,000 g/mol= 3.92 x 10^{-13} M. Given a reported dissociation constant Kd=10^{-9} M (Torres et al., 1995), we observed a maximal concentration of IFN-γ in our EV preparations that was 2500 times lower than the theoretical concentration required to bind half the IFN-γ receptors on NIH 3T3 cells. We also tested the levels of Stat1 activation in NIH 3T3 cells treated with Th1 cytokines or IFN-γ only, at 10-fold serial dilutions. The maximal concentration of IFN-γ found in 6 x 10^6 NPC-derived EVs was 7.05 pg/ml, which corresponds to

around 10^{-4}x of the working concentration used to treat NPCs (1x= IFN-γ 100 ng/ml, TNF-α 20 ng/ml, IL1-β 0.2 ng/ml). Based on WB analysis for Stat1 pathway, all the three forms of Stat1 - total, pStat1(Y701), pStat1(S727) - showed a dose-dependent activation in response to the treatment with Th1 cytokines. At a 10^{-3}x dilution, corresponding to a concentration of IFN-γ of 100 pg/ml (10 times more than the cytokine level detected in EVs), both the phosphorylated forms were undetectable, while the levels of total Stat1 undistinguishable from the untreated control cells (**Figure S12**). Furthermore, knowing that NIH 3T3 cells expressed receptors for IL-4, IL-5 and IL-13 from flow cytometry analysis (**Figure S2**), we also performed the parallel control experiment with 10-fold dilutions of the Th2 mix, staining for Stat6 and pStat6 (Figure S12). pStat6 showed a dose dependent activation to increasing concentrations of Th2 cytokines. The total levels of Stat6 did not show any alteration in any of the tested samples. However, Th2 EVs did not induce any detectable activation of Stat6, once again confirming the specificity of Th1 vesicles in inducing a response in NIH 3T3 cells. Therefore, we concluded that the Th1 specific response detected in NIH 3T3 cells was not determined by cytokine contamination, but rather was a specific effect mediated by EVs enriched with the IFN -γ/Ifngr1 complex.

Estimation of the half life of the IFN- γ/Ifngr 1 complex

Table. Reported dissociation constants for the IFN- γ/Ifngr 1 interaction.

K_D	Cell type	k_{on}	k_{off}	References
1 x 10^{-9} M	Oligodendrocyte			(Torres et al., 1995)
1.64 x 10^{-9} M	Astrocyte			(Rubio and de Felipe, 1991)
3 x 10^{-10} M	Lymphocyte			(Bomsztyk et al., 1989)
2 x 10^{-10} M	Raji			(Fountoulakis et al., 1989)
1.3 x 10^{-10} M	HeLa			(Fischer et al., 1988)
1 x 10^{-10} M	Monocytes			(Fischer et al., 1988)
3.18 x 10^{-10} M*	n.a. (sensor chip)	1.57 x 10^{7} M^{-1} s^{-1}	5 x 10^{-3} s^{-1}	(Sadir et al., 1998)

* Parameters reported are those based on the highest k_{on} rate measured in the reference.

A very small dissociation constant (K_D) is indeed indicative of a high-affinity association, thus it is a fair assumption that at any given moment a significantly large fraction of the ligand is bound to its appropriate receptor (the exact percentage bound dependent on the concentrations of the ligand and receptor). However, the nature of non-covalent interactions is such that this interaction, while long-lived on a biological timescale (i.e. long-enough to trigger appropriate cellular signalling responses), is transient. The kinetics of the interaction are such that $K_D = k_{off} / k_{on}$, where k_{off} is the

unimolecular rate of the dissociation of the ligand-receptor (i.e. IFN-γ/Ifngr1) complex (in M^{-1}), while k_{on} is the bimolecular rate of complex formation (M^{-1} s^{-1}).

Sadir et al. measured the kinetic parameters (k_{off} and k_{on}) of the IFN-γ/Ifngr1 association using surface plasmon resonance. While this is only a model of the biological system (i.e. using a sensor chip-immobilised analogue of the surface Ifngr1 epitope rather than the actual membrane-bound receptor), the K_D value ascertained reflects those determined for IFN-γ/Ifngr1 interactions in a number of other studies across several cell types. Moreover, the calculated k_{on} rate falls within the typically expected range for protein-protein interactions (10^4-10^8 M^{-1} s^{-1}) (Archakov et al., 2003; Northrup and Erickson, 1992).

Higher rates can be expected in stronger electrostatic attractions, however an upper diffusion-limited rate constant is expected at 10^9-10^{10} M^{-1} s^{-1}, as described by the Smoluchowski expression (Schlosshauer and Baker, 2004).

Using the k_{off} value it is possible to calculate the half-life ($t_{1/2}$) of the IFN-γ/Ifngr1 complex as a first order reaction:

$$t_{1/2} = \ln 2/k_{off}$$

From the k_{off} value of Sadir et al. (5×10^{-3} s^{-1}), the half-life of the IFN-γ/Ifngr1 complex is found to be 139 seconds. Thus, approximately every two minutes half of the IFN-γ/Ifngr1 complexes dissociate, with the now-free IFN-γ able to be sequestered by another IFN-γ receptor. Similar half-lives (several minutes maximum) are obtained using k_{off} values calculated from other reported K_D values and k_{on} values in the typically accepted range.

As the IFN-γ-bearing EVs are incubated in the presence of target cells for 24 hours, this would seem to be ample time for IFN-γ released from an EV to equilibrate between EV- and cell-based IFN-γ receptors. Furthermore, it is envisaged that as cellular Ifngr1 -bound IFN-γ is removed from the medium via rapid internalisation of the IFN-γ receptor ($t_{1/2}$ = 4-5 minutes in cultured fibroblasts) (Anderson et al., 1983), additional IFN-γ will be released from EV-associated Ifngr1 in an effort to maintain equilibrium as per:

$$\text{IFN-}\gamma + \text{Ifngr1} \rightleftarrows \text{IFN-}\gamma\text{-Ifngr1}$$

$$K_D = [\text{IFN-}\gamma]\,[\text{Ifngr1}] / [\text{IFN-}\gamma\text{-Ifngr1}]$$

EV-associated Ifngr 1-bound IFN-γ is not internalised in such manner, and so it remains available for release into the medium and binding to other receptors.

Statistical Analysis

For qRT-PCR: Data have been analysed with the 2-ΔΔCT method, normalising over GAPDH expression and reporting the data as a fold change over NIH 3T3 cells not exposed to EVs. Statistical analysis: One-way Anova with Tukey Honest Significant Difference post-hoc test against NIH 3T3 cells exposed to Basal EVs.

For ELISA: One-way Anova with Bonferroni's multiple comparison post-hoc test against NIH 3T3 not exposed to EVs.

Supplemental References

Anderson, P., Yip, Y.K., and Vilcek, J. (1983). Human interferon-gamma is internalized and degraded by cultured fibroblasts. J Biol Chem *258*, 6497-6502.

Archakov, A.I., Govorun, V.M., Dubanov, A.V., Ivanov, Y.D., Veselovsky, A.V., Lewi, P., and Janssen, P. (2003). Protein-protein interactions as a target for drugs in proteomics. Proteomics *3*, 380-391.

Artavanis-Tsakonas, K., Love, J.C., Ploegh, H.L., and Vyas, J.M. (2006). Recruitment of CD63 to Cryptococcus neoformans phagosomes requires acidification. Proc Natl Acad Sci U S A *103*, 15945-15950.

Bomsztyk, K., Stanton, T.H., Smith, L.L., Rachie, N.A., and Dower, S.K. (1989). Properties of interleukin-1 and interferon-gamma receptors in B lymphoid cell line. J Biol Chem *264*, 6052-6057.

Cox, J., and Mann, M. (2008). MaxQuant enables high peptide identification rates, individualized p.p.b.-range mass accuracies and proteome-wide protein quantification. Nat Biotechnol *26*, 1367-1372.

Durbin, J.E., Hackenmiller, R., Simon, M.C., and Levy, D.E. (1996). Targeted disruption of the mouse Stat1 gene results in compromised innate immunity to viral disease. Cell *84*, 443-450.

Fischer, D.G., Novick, D., Orchansky, P., and Rubinstein, M. (1988). Two molecular forms of the human interferon-gamma receptor. Ligand binding, internalization, and down-regulation. J Biol Chem *263*, 2632-2637.

Follenzi, A., Ailles, L.E., Bakovic, S., Geuna, M., and Naldini, L. (2000). Gene transfer by lentiviral vectors is limited by nuclear translocation and rescued by HIV-1 pol sequences. Nat Genet *25*, 217-222.

Fountoulakis, M., Kania, M., Ozmen, L., Loetscher, H.R., Garotta, G., and van Loon, A.P. (1989). Structure and membrane topology of the high-affinity receptor for human IFN-gamma: requirements for binding IFN-gamma. One single 90-kilodalton IFN-gamma receptor can lead to multiple cross-linked products and isolated proteins. J Immunol *143*, 3266-3276.

Huang, S., Hendriks, W., Althage, A., Hemmi, S., Bluethmann, H., Kamijo, R., Vilcek, J., Zinkernagel, R.M., and Aguet, M. (1993). Immune response in mice that lack the interferon-gamma receptor. Science *259*, 1742-1745.

Kreutzfeldt, M., Bergthaler, A., Fernandez, M., Bruck, W., Steinbach, K., Vorm, M., Coras, R., Blumcke, I., Bonilla, W.V., Fleige, A.*, et al.* (2013). Neuroprotective

intervention by interferon-gamma blockade prevents CD8+ T cell-mediated dendrite and synapse loss. J Exp Med *210*, 2087-2103.

Livak, K.J., and Schmittgen, T.D. (2001). Analysis of relative gene expression data using real-time quantitative PCR and the 2(-Delta Delta C(T)) Method. Methods *25*, 402-408.

Mostafavi, S., Ray, D., Warde-Farley, D., Grouios, C., and Morris, Q. (2008). GeneMANIA: a real-time multiple association network integration algorithm for predicting gene function. Genome biology *9 Suppl 1*, S4.

Northrup, S.H., and Erickson, H.P. (1992). Kinetics of protein-protein association explained by Brownian dynamics computer simulation. Proc Natl Acad Sci U S A *89*, 3338-3342.

Pluchino, S., Muzio, L., Imitola, J., Deleidi, M., Alfaro-Cervello, C., Salani, G., Porcheri, C., Brambilla, E., Cavasinni, F., Bergamaschi, A.*, et al.* (2008). Persistent inflammation alters the function of the endogenous brain stem cell compartment. Brain *131*, 2564-2578.

Rubio, N., and de Felipe, C. (1991). Demonstration of the presence of a specific interferon-gamma receptor on murine astrocyte cell surface. J Neuroimmunol *35*, 111-117.

Sadir, R., Forest, E., and Lortat-Jacob, H. (1998). The heparan sulfate binding sequence of interferon-gamma increased the on rate of the interferon-gamma-interferon-gamma receptor complex formation. J Biol Chem *273*, 10919-10925.

Schlosshauer, M., and Baker, D. (2004). Realistic protein-protein association rates from a simple diffusional model neglecting long-range interactions, free energy barriers, and landscape ruggedness. Protein science : a publication of the Protein Society *13*, 1660-1669.

Shevchenko, A., Wilm, M., Vorm, O., and Mann, M. (1996). Mass spectrometric sequencing of proteins silver-stained polyacrylamide gels. Analytical chemistry *68*, 850-858.

Torres, C., Aranguez, I., and Rubio, N. (1995). Expression of interferon-gamma receptors on murine oligodendrocytes and its regulation by cytokines and mitogens. Immunology *86*, 250-255.

Trapnell, C., Roberts, A., Goff, L., Pertea, G., Kim, D., Kelley, D.R., Pimentel, H., Salzberg, S.L., Rinn, J.L., and Pachter, L. (2012). Differential gene and transcript expression analysis of RNA-seq experiments with TopHat and Cufflinks. Nat Protoc *7*, 562-578.

Warde-Farley, D., Donaldson, S.L., Comes, O., Zuberi, K., Badrawi, R., Chao, P., Franz, M., Grouios, C., Kazi, F., Lopes, C.T.*, et al.* (2010). The GeneMANIA prediction server: biological network integration for gene prioritization and predicting gene function. Nucleic Acids Res *38*, W214-220.